ELSEVIER

Fusion Engineering and Design 63–64 (2002) 397–403

Fusion Engineering and Design

www.elsevier.com/locate/fusengdes

Experimental study of turbulent supercritical open channel water flow as applied to the CLiFF concept

S. Smolentsev *, B. Freeze, N. Morley, M. Abdou

Fusion Science and Technology Group, Department of Mechanical and Aerospace Engineering, UCLA, 420 Westwood Plaza, 44-114 Engineering IV, Box 951597, Los Angeles, CA 90095-1597, USA

Abstract

An experimental study of turbulent open channel water flows was conducted that simulated basic features of the flow of molten salt in the convective liquid flow first-wall (CLiFF) concept, which is a part of the Advanced Power Extraction (APEX) study. Unlike many other studies of open channel flows, the present one concentrates on a supercritical flow regime, in which surface waviness and wave–turbulence interaction are the most important processes that determine the heat transfer rate in CLiFF flows. The current study covers the Reynolds number and Froude number range of 1×10^4–6×10^4 and 150–250, respectively, with a fixed chute inclination angle of 30°. The statistical characteristics of the wavy interface were obtained with an ultrasound transducer. A spectral analysis of the oscillating flow thickness shows that a major part of the spectrum is presented by long finite-amplitude waves ($f = 10$–50 Hz), which carry a significant part of the volumetric flux. Based on dye technique observations, short waves are mostly responsible for mixing the liquid at the surface. The surface waviness can be characterized by a parameter built through the mean flow thickness, h, and its standard deviation (S.D.), σ, as $0.5\sigma/h$, which is almost constant, 0.1, in all experiments. The mean flow thickness variations are predicted well with the 'K–ε' model of turbulence [Int. J. Eng. Sci. 40/6 (2002) 693], but the fluctuations are not resolved. Thermal images of the free surface measured by an infrared (IR) camera are very non-uniform and show the 'strike' structures in the form of elongated strips of 'hotter' and 'cooler' liquid. The present observations are the first steps to better understanding and quantitative predictions of liquid wall flows in the CLiFF design.

Keywords: APEX; Liquid wall; Low conductivity fluid; Turbulence; Surface waves; Heat transfer

1. Introduction

In fusion cooling applications, high heat capacity, high thermal conductivity media such as liquid metals are traditionally assumed to be the best working fluid. However, due to their high electrical conductivity ($\sim 10^6\ \Omega^{-1}\ \mathrm{m}^{-1}$), liquid metals have strong magnetohydrodynamic (MHD) interaction when flowing across the reactor magnetic field, which can result in a high MHD drag, as well as turbulence suppression. Along with liquid metals, molten salts are being considered as a coolant in plasma-facing components. For

* Corresponding author. Tel.: +1-310-794-5366; fax: +1-310-825-2599

E-mail address: sergey@fusion.ucla.edu (S. Smolentsev).

0920-3796/02/$ - see front matter
PII: S0920-3796(02)00121-7

example, free surface flows of molten salts, such as Flibe (and recently Flinabe), are intensively studied in the Advanced Power Extraction (APEX) project [1]. Unlike liquid metals, molten salts have a much lower electrical conductivity ($\sim 10^2\ \Omega^{-1}\ m^{-1}$) and poor thermal conductivity. Thus, they do not experience strong MHD forces and to a large extent remain turbulent, but their heat transfer capabilities are sufficiently poorer than those of liquid metals. Therefore, a practical question is whether or not turbulent mixing in molten salts is sufficiently high enough to tolerate high heat loads. As a particular design that potentially can accommodate molten salts as a coolant, we will refer to the convective liquid flow first-wall (CliFF) concept, which is a part of the APEX study. In CLiFF, the liquid flows poloidaly over an 8 m first-wall section from the chamber top to bottom, forming a liquid layer with a thickness of about 2 cm, and the velocity of about 10 m s^{-1} [1]. The free surface is imposed to a high heat flux (~ 2 MW m^{-2}) from the surrounding plasma. The primary goal of the present study is to investigate the hydrodynamic and heat transfer phenomena in the near-surface region of a turbulent open channel flow, heated from the free surface by experimentally simulating the conditions similar to those in the CLiFF concept.

2. Background

The surface heat transfer in the reference case depends mostly on two different mechanisms. First, heat transfer degradation may take place due to suppression of turbulent pulsations through Joule dissipation. This mechanism affects the whole flow region and has an impact on both near-wall and near-surface turbulence. Turbulence reduction by a magnetic field in open channel flows has been studied numerically [2,3] on the basis of the 'K–ε' model of turbulence. The second mechanism, which probably affects the turbulent transport across the interface to a much larger extent, is related to specific phenomena in the near-surface region. These include 'surface renewal', turbulence kinetic energy redistribution, generation of turbulence by wind shear, and wave–turbulence interaction. Many, but not all, aspects of these phenomena were studied experimentally [4–7] and numerically [8–10] using DNS. For a review of different approaches, see [11,12].

Based on these studies of turbulent structures in open channel flows, one can distinguish three typical situations, which are referred to here as a 'gas–liquid interface with a high shear rate', 'gas–liquid interface with a low shear rate', and 'supercritical flow'. Perhaps the most frequently analyzed case is related to the gas–liquid interface with a high shear rate. In this case, organized low speed/high speed 'streaky' structures are observed that periodically break down into 'bursts'. Qualitatively, this phenomenon does not differ from that at solid walls for the same shear rate [11]. At low shear rates, the structures observed are 'patchy' and appear to arise from turbulence generated in the near-wall region. Typically, these two situations are analyzed under conditions that correspond to subcritical flows ($Fr < 1$), which indicates non-amplification of the surface waves. Unlike subcritical flows, in supercritical flows ($Fr > 1$) any disturbance in the flow can grow, finally resulting in a wavy interface. A good illustration of supercritical flow is a falling film that demonstrates a whole spectrum of non-linear, three-dimensional surface waves. This phenomenon is not fully understood. If heat (or mass) flux is applied to the free surface, the intensity of the scalar transport across the interface will depend strongly on the turbulence structures in the near-surface region and their interaction with the waves.

Returning to the CLiFF concept, both Froude numbers, $Fr_\perp$ and $Fr_\parallel$, built through the normal and tangential component of $\mathbf{g}$, respectively, are much higher than unity. This implies a supercritical flow regime in the CLiFF flow. Moreover, a specific feature of the CLiFF flow is that the free surface is not imposed to any shear from a surrounding medium and, hence, no turbulence is generated at the interface due to wind shear. At the same time, however, turbulence at the surface can be produced by the waves themselves. This will also affect the heat transfer rate. The magnitude of the effect of the surface waves on heat transfer along with the physical mechanism behind this

effect requires further clarification. These particular questions have been addressed with the experimental facilities described below.

3. Experiment

The experiments were conducted using the Flibe Hydrodynamics (FliHy) loop (Fig. 1) described in [13]. Hence, only a very brief description is given here. The test section is a 4 m long, 40 cm wide inclined chute. The working fluid (currently water) is injected continuously into the test section by two centrifugal pumps (up to 75 l s^{-1}), connected in parallel through an adjustable nozzle (3–50 mm height). The nozzle has a honeycomb and a secondary screen to reduce the inlet turbulence. The nozzle height is adjusted to provide an inlet flow thickness as close to the equilibrium one as possible. This reduces the transition length significantly. The liquid is collected into a 1 m^3 tank at the bottom of the supporting frame. An infrared (IR) heater (30×30 cm, up to 60 kW m^{-2}) located 3.5 m down from the nozzle is used to heat the liquid from the side of the free surface. All measurements are conducted right after the heated area, where the flow is fully developed. The measurements include the IR images by the FLIR-600 IR camera, and the flow thickness versus time by an ultrasound transducer. A dye technique is also used to visualize the free surface structure.

In the experiments, the flow rate, the inclination angle, and the nozzle height can be changed to provide a wide range of dimensionless flow parameters, such as the Reynolds number ($Re = U_m h/\nu$) and Froude number ($Fr = U_m^2/\mathbf{g}h$). This range corresponds to that in CLiFF. Currently, $Re = 1 \times 10^4$–6×10^4, and $Fr = 150$–250. At the same time, the speed of the liquid in almost all experiments is not too high (typically 2–5 m s^{-1}) and the surrounding air is stagnant, such that only a low shear rate can be produced at the interface. Thus, the flow conditions similar to those in CLiFF are provided. The experimental facilities do not have special tools to completely eliminate the air entrainment effect. However, photographs of the flow, as well as visual observations, have not revealed any air bubbles in the water. Splashing water has not been observed either. Visual observations show much more waviness at the surface as the flow rate and/or the inclination angle grow. Directly at the nozzle, the free surface is smooth, the surface waves grow in amplitude downstream reaching a quasi-saturation state over some distance (1–2 m) from the nozzle, which varies depending on the flow parameters. Experiments with a red dye injected tangentially to the free surface show that the dye disappears from the

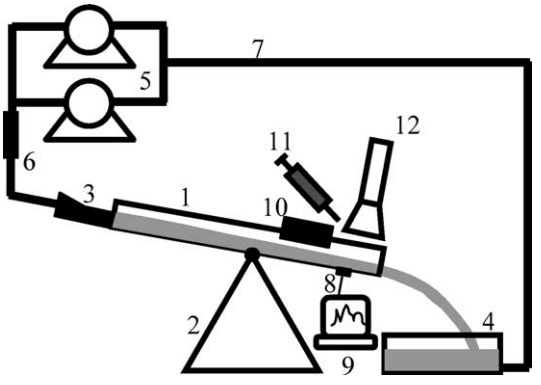

Fig. 1. Schematic of experimental equipment, (1) inclined test-section; (2) frame; (3) nozzle; (4) tank; (5) two pumps; (6) flow-meter; (7) hoses; (8) ultrasound transducer; (9) PC; 10-IR heater; (11) dye injector; (12) IR camera.

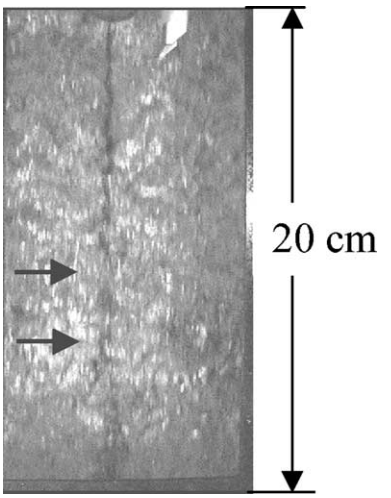

Fig. 2. Free surface visualization using a red dye. The arrows show locations at the surface where the dye disappears.

free surface and reappears again when propagating downstream (Fig. 2), which is a very clear indication of overturning waves. The overturning waves occur on the scale of the flow thickness.

4. Statistical characteristics of the wavy free surface

The variations of the flow thickness versus time at a given point within a fully developed flow section measured with the ultrasound transducer are shown in Fig. 3. The curve, $h(t)$, is based on 509 subsequent measurements of the flow thickness taken with a time increment of 1 ms. Since the flow is inherently unstable, the oscillations appear to be due to the growth of initially small flow perturbations in the nozzle, near the side walls, or can be caused by interaction of the bulk vortices with the free surface.

A spectral analysis was applied to the $h(t)$ data. The goal of the spectral analysis is to estimate the distribution (over frequency) of the power contained in a signal. First, the original $h(t)$ data were filtered using a Gaussian low-pass filter to cut a high frequency component that reduces the spectrum noise. An advantage of the Gaussian filter, over other commonly used digital filters, is that it annihilates all Fourier modes of wave-number $|k|$ greater than the cut-off wave-number, whereas it has no effect on lower wave-number modes. The cut-off parameter in the Gaussian filter function was chosen in such a way to cut all frequencies higher than 250 Hz (the preliminary analyses based on the unfiltered data showed that such frequencies are insignificant). After filtering, Welch's averaged periodogram method [14] is applied to estimate the power spectral density (PSD). However, applying this procedure to a single data set results in a PSD, which resembles a pure noise. This is because there is not enough information in the original 509 points to obtain a well-behaved curve. To reduce the spectral noise, many more data sets were used. Each data set was treated in the same way as described above. The resulting frequency spectra were then averaged to form a single frequency spectrum. As a result of this procedure, the spectrum noise has been reduced in proportion to the square root of the number of the data sets, to a level that allows interesting features to be resolved (Fig. 4). This obtained PSD that utilized 50 data sets is rather smooth and demonstrates two large peaks at about 10–15 and 30–40 Hz, as well as a long 'tail' of higher frequency modes. If one takes the bulk velocity, U_m, as a first approximation to the wave propagation speed, c, one can estimate the wavelengths corresponding to the peaks ($\lambda_{peak} = 2\pi c/$

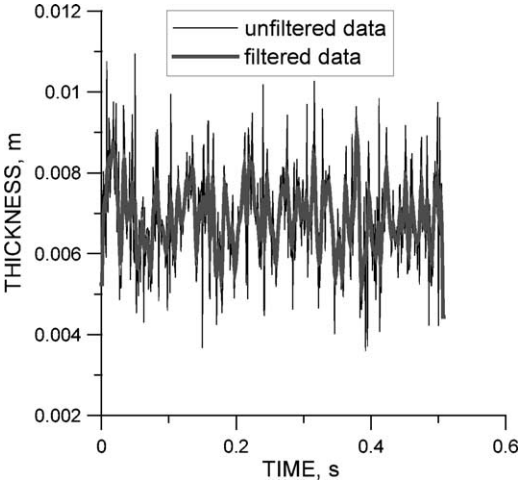

Fig. 3. Time variations of the flow thickness in a given point within the fully developed flow section.

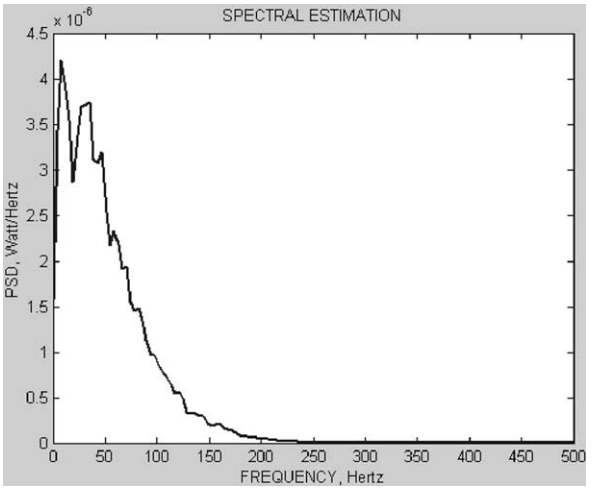

Fig. 4. Typical spectrum of $h(t)$ based on the averaging of 50 data sets.

f_{peak}) as about 1 m and 0.5 m, respectively. At the same time, the dye technique images (Fig. 2) show that the overturning waves, which are responsible for mixing the liquid at the surface, occur at much smaller scales, comparable to the flow thickness. Based on these two observations, one can conclude that the long waves transport a significant fraction of the volumetric flux, while the shorter waves determine scalar transport across the interface.

The mean flow thickness versus Reynolds number, along with a waviness parameter, is illustrated by Fig. 5. The waviness parameter is defined here as half of the S.D., $\Delta h = 0.5\sigma$, and is a good representation of the degree of waviness. Since the value of this parameter is comparable to the flow thickness, the waves observed should be classified as finite-amplitude waves. One can see that the surface waviness grows as the flow thickness grows with Re. In Fig. 6, the data for the waviness parameter from Fig. 5 are plotted in the form of $\Delta h/h$, as a function of Re and Fr. Although both Re and Fr vary in a wide range, the quantity $\Delta h/h$ slightly decreases from about 0.11–0.09. Such a tendency can serve as a reasonable argument to treat $\Delta h/h$ as a type of the flow invariant.

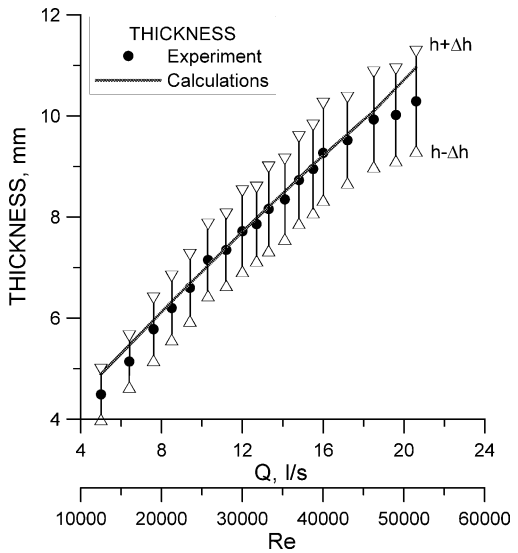

Fig. 5. Mean flow thickness and waviness parameter within the fully developed flow section.

5. Application of the '$K-\varepsilon$' model to calculations of the flow thickness

Since both the flow length in CLiFF and the expected characteristic free surface wavelengths are much higher than the flow thickness, it is unlikely that DNS or even LES can be applicable to the CLiFF design in the near future, because of the present computational speed and memory limitations. Unlike DNS and LES, RANS models have much lower computational requirements and their applicability to the CLiFF-type flows has not been limited by a computational cost. As a matter of fact, the RANS models remain the only CFD tools suited for modeling flows in CLiFF. However, RANS models resolve only the mean flow and do not allow the high spatial and temporal resolution of turbulent flows that would be accessible with DNS or LES. Thus, the limitations of the RANS models when applying to the CLiFF design should be clarified. In the present study, the low Reynolds number '$K-\varepsilon$' model [2] was applied to calculate the downstream variations of the flow thickness and, then, the calculated results were compared against the actual flow thickness as measured in the present experiment. As was expected, no surface waviness was observed in the calculations, because the '$K-\varepsilon$' model is too dissipative. However, the model predicts the mean flow thickness very well, as is evident from Fig. 5.

6. Heat transfer

A typical thermal image of the free surface, right after the flow exits the lower heater edge region, taken with the IR camera, is shown in Fig. 7. The temperature field is essentially non-uniform. One can see temperature 'strikes' in the form of elongated strips of 'hotter' and 'cooler' liquid. Such structures result from complex, non-linear waves and wave–turbulence interaction. Analysis of the heat transfer rate across the wavy interface and its correlation with the hydrodynamic turbulence structures depending on the flow parameters is under progress. Corresponding results will be presented in future publications.

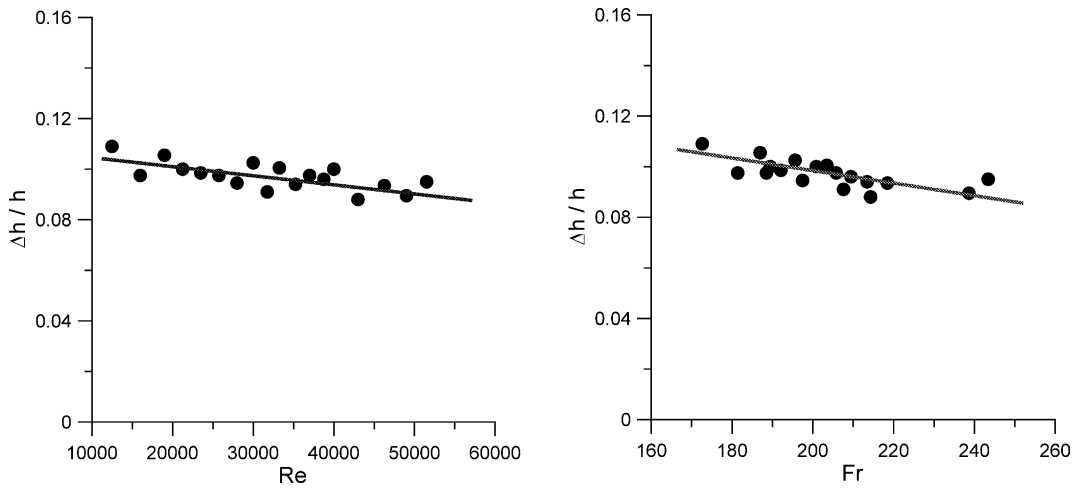

Fig. 6. Dimensionless waviness parameter as a function of *Re* (left) and *Fr* (right).

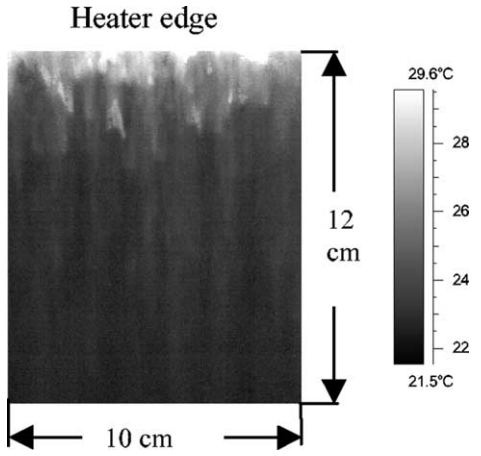

Fig. 7. Thermal image of the free surface.

7. Concluding remarks

The experiments conducted show a complicated wave phenomena at the free surface. Finite-amplitude surface waves having a wide spectrum of low (10–50 Hz) and high (up to 250 Hz) frequencies significantly affect both near-surface hydrodynamics and heat transfer. Future studies will concentrate on further quantification of these phenomena and implementation of the experimental data into the '$K-\varepsilon$' model through proper adjustment of the turbulence Prandtl number. The effect of a magnetic field on the surface waviness in electrically conducting fluids will also be studied.

Acknowledgements

The authors would like to acknowledge the support of the APEX project through DOE Grant DE-FG03-86ER52123. The first author would like to express his gratitude to Professor Tomoaki Kunugi from Kyoto University, Japan for his valuable comments and discussions.

References

[1] M.A. Abdou, The APEX TEAM, On the exploration of innovative concepts for fusion chamber technology, Fusion Eng. Des. 54 (2001) 181–247.
[2] S. Smolentsev, M. Abdou, N. Morley, A. Ying, T. Kunugi, Application of the '$K-\varepsilon$' model to open channel flows in a magnetic field, Int. J. Eng. Sci. 40/6 (2002) 693–711.
[3] S. Smolentsev, M. Abdou, T. Kunugi, N. Morley, S. Satake, A. Ying, Modeling of liquid walls in APEX study, Int. J. Appl. Electromagn. Mech. (2002), in press.
[4] H. Ueda, R. Moller, S. Komori, T. Mizushina, Eddy diffusivity near the free surface of open channel flow, Int. J. Heat Mass Transfer. 20 (1977) 1127–1136.

[5] S. Komori, H. Ueda, Turbulence structure and transport mechanism at the free surface in an open channel flow, Int. J. Heat Mass Transfer. 25 (1982) 513–521.
[6] S. Komori, Y. Murakami, H. Ueda, The relationship between surface-renewal and bursting motions in an open channel flow, J. Fluid Mech. 203 (1989) 103–123.
[7] M. Rashidi, Burst-interface interactions in free surface turbulent flows, Phys. Fluids 9 (1997) 3485–3501.
[8] S. Komori, R. Nagaosa, Y. Murakami, S. Chiba, K. Ishii, K. Kuwahara, Direct numerical simulation of three-dimensional open-channel flow with zero-shear gas–liquid interface, Phys. Fluids A5 (2) (1993) 115–125.
[9] V. De Angelis, Numerical investigation and modeling of mass transfer processes at sheared gas–liquid interfaces, Ph.D. dissertation, UCSB, 1998, p. 151.
[10] Y. Yamamoto, T. Kunugi, A. Serizawa, Turbulence statistics and scalar transport in an open-channel flow, J. Turbulence (http://jot.iop.org/), 2, 010 (2001).
[11] S. Banerjee, Turbulence structure and transport mechanisms at interfaces, Proceeding of the Ninth International Heat Transfer Conference, vol. 1, 1990, pp. 395–418.
[12] S. Banerjee, Upwellings, downdrafts, and whirpools: dominant structures in free surface turbulence, Appl. Mech. Rev. 6 (2) (1994) 166–172.
[13] B. Freeze, M. Dagher, T. Sketchley, N. Morley, S. Smolentsev, M. Abdou, FliHy experimental facilities for studying open channel turbulent flows and heat transfer, ISFNT-6, San Diego, Fus. Eng. Des., Vol 61–64, 2002.
[14] T. Saa, in: S.K. Mitra, J.F. Kaiser (Eds.), Handbook for Digital Signal Processing, Willey, 1993, p. 1268.